



HAL
open science

MORPHOLOGICAL CHARACTERIZATION OF DROPLETS. APPLICATION TO ATOMIZATION OF SPRAYS

Nicolas Fdida, Jean-Bernard Blaisot

► **To cite this version:**

Nicolas Fdida, Jean-Bernard Blaisot. MORPHOLOGICAL CHARACTERIZATION OF DROPLETS. APPLICATION TO ATOMIZATION OF SPRAYS. 13th International Symposium on Flow Visualization, Jul 2008, Nice, France. <hal-05520917>

HAL Id: hal-05520917

<https://hal.science/hal-05520917v1>

Submitted on 1 Apr 2026

HAL is a multi-disciplinary open access archive for the deposit and dissemination of scientific research documents, whether they are published or not. The documents may come from teaching and research institutions in France or abroad, or from public or private research centers.

L'archive ouverte pluridisciplinaire HAL, est destinée au dépôt et à la diffusion de documents scientifiques de niveau recherche, publiés ou non, émanant des établissements d'enseignement et de recherche français ou étrangers, des laboratoires publics ou privés.



Distributed under a Creative Commons CC BY-NC-ND 4.0 - Attribution - Non-commercial use - No Derivative Works - International License



MORPHOLOGICAL CHARACTERIZATION OF DROPLETS. APPLICATION TO ATOMIZATION OF SPRAYS.

Nicolas Fdida*, Jean-Bernard Blaisot*

*CORIA/UMR-6614, CNRS, Université et INSA de Rouen,
Avenue de l'Université, 76801 Saint Etienne du Rouvray, FRANCE

KEYWORDS:

Main subject(s): *Atomization*

Fluid: *Spray, Drop-sizing, Droplet Morphology*

Visualization method(s): *Shadow Imaging*

ABSTRACT : *In many industrial applications, a given mass of a liquid is sprayed by an injector in a carrier gas in order to maximize the mass or heat exchange flux between the liquid and the gas by increasing the liquid-gas interface area. The atomization process is a rather complex phenomenon that comprises at least two stages: the primary and the secondary atomization process.*

The characteristics of a spray are often given by the measurement of the drop size distribution. The main features of this distribution are represented by mean diameters. The underlying hypothesis is that all liquid elements are spherical. Of course, such an ideal case is not the rule and could only occur at the final stage of the evolution of a spray. There is so a need for new description tools better fitted to not fully atomized sprays.

In this study, we define 4 morphological parameters in order to characterize various droplet shapes. We choose particular objects such as ellipses or Cassini ovals to simulate drops in the atomization state. We analyze the distribution of the droplets of a real spray in the planes defined by those shape parameters.

1 Introduction

In many industrial applications, a given mass of a liquid is sprayed by an injector in a carrier gas in order to maximize the mass or heat exchange flux between the liquid and the gas by increasing the liquid-gas interface area. The atomization process is a rather complex phenomenon that comprises at least two stages. During the primary atomization, the continuous liquid phase breaks up in fragments. Additional atomization of these fragments into smaller droplets constitutes the secondary atomization process.

The characteristics of a spray are often given by the measurement of the drop size distribution. The main features of this distribution are represented by mean diameters. The underlying hypothesis is that all liquid elements are spherical. Of course, such an ideal case is not the rule and could only occur at the final stage of the evolution of a spray. There is so a need for new description tools better fitted to not fully atomized sprays.

We propose in this paper a tool based on the characterization of the shape of the drops. Morphological criteria are defined to classify droplets, which belong to different kind of shape families such as

spherical, elliptical, and Cassini oval families. A shadow-imaging technique is used to visualize drops in a spray. The contours of the droplet images are computed in a way to obtain sub-pixel accuracy. Four shape parameters are defined from sub-pixel contours.

2 Definition of the shape parameters

2.1 Shape Characterization of Droplets

Imaging techniques are based on the measurement of the 2-D projection of a 3-D object. Thus, the image of a droplet in a spray gives a surface distribution of the liquid in the gas. This can give us shape criteria associated to each droplet. The choice of such a criterion is not obvious because of the particular shape of a drop whose edges are fragments of arc of a circle. N.Chigier[1] counts sixteen parameters for particle characterization (see Table 1). All those parameters are based on quantities given in Fig.1. Five parameters are related to the diameter of the particle and five to its surface. The last six are considered as shape parameters because they are dimensionless as the Z parameter, defined as a ratio of a perimeter equivalent diameter to an area equivalent diameter. It can be understood as the ratio of the actual perimeter to that of a circle having the same area as the measured area. Among those shape parameters, only EF and DF are based on a surface ratio, which may give them a strong hardness. Indeed the error due to the pixel count is bigger on perimeter than on surface measurements. Actually, the parameters EF and DF are based on length measurements and depend on the orientation of the particle in the image. To avoid this problem, Malot & Blaisot[2] proposed a new parameter, the Sphericity S_p , independent of the orientation, and related to the projected area of the particle.

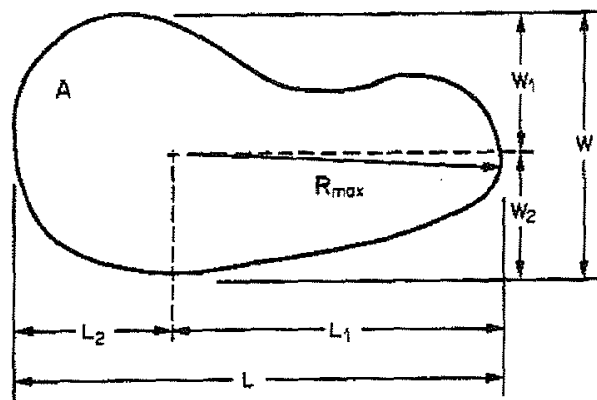


Fig.1. Characterization of the shape of a droplet [1]

Most authors only considered morphology parameters to sort spherical and non-spherical droplets, as Malot & Dumouchel[3]. This is due to the fact that most of optical instruments for drop-sizing, such as diffraction-based drop-sizer or Phase Doppler Particle Analysers (PDA) are based on the hypothesis of spherical particles whereas the drop shapes can also be analyzed by the Imaging technique. However, the rapid developments in Imaging Techniques needed to grow on by comparing its results with those established techniques. That's why sphericity criteria needed to be found. In this study we want to point out the main advantage of Imaging Techniques: the characterization of the shape of different kind of droplets by defining several morphological parameters.

	<i>Symbol</i>	<i>Name</i>	<i>Expression</i>
Diameters	D_A	Area equivalent diameter	$\sqrt{(4.A/\pi)}$
	D_P	Perimeter equivalent diameter	P/π
	D_{AP}	Diameter for equivalent area/perimeter	$4.A/P$
	D_{LW}	Arithmetic mean diameter	$(L + W)/2$
	D_{max}	Maximum diameter	$2.R_{max}$
Areas	A_P	Perimeter equivalent area	$P^2/4.\pi$
	A_{AP}	Area for equivalent area/perimeter	$4.\pi.A^2/P^2$
	A_{max}	Maximum area	$\Pi.R^2_{max}$
	A_R	Rectangular area	$L.W$
	A_E	Elliptical area	$\pi.L.W/4$
Shape Factors	Z	Irregularity factor	D_P/D_A
	EF	Ellipse factor	A_E/A
	DF	Density factor	A/A_{max}
	R	Ansiometry factor	L/W
	AFW	Symmetry factor	L_1/L_2
	AFL	Symmetry factor	W_1/W_2

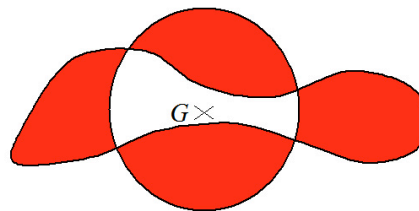
Table 1. Parameters for particle characterization [1]

2.2 Sphericity S_p

Sphericity and Irregularity (see below) parameters are based on the equivalent disc, i.e. the disc having the same area than the object and centered on the gravity centre of the object. The Sphericity S_p is defined by Eq. (1). It corresponds to the ratio of the difference between the union and the intersection of the surface S of the particle and the surface S_C of the equivalent disc and the surface S of the particle. It can be seen as the ratio of the colored surface on the Fig.2 to the surface of the particle S . This ratio is null in the case of a sphere and limited to 2 for elongated shapes.

$$S_p = \frac{A(S \cup S_C) - A(S \cap S_C)}{A(S)} \quad (1)$$

In Eq.1, $A(x)$ stands for the area of surface x . High values of S_p refers to chains of droplets or ligaments in general.


Fig.2. Definition of the Sphericity S_p

2.3 Ellipticity ε

The Ellipticity ε is the ratio of the maximum length L_{max} along the inertial axis of the particle image to the minimum length L_{min} perpendicularly to this inertial axis (See Fig.3). This parameter ranges between 0 and 1. It is equal to 1 for a disc.

$$\varepsilon = \frac{L_{min}}{L_{max}} \quad (2)$$

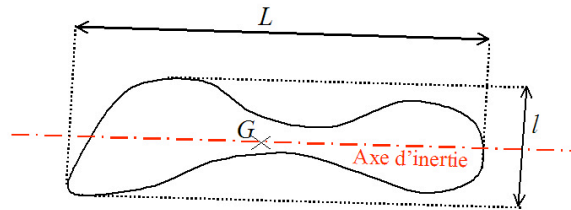


Fig.3. Definition of the Ellipticity ε

2.4 Irregularity φ

The Irregularity φ is defined as ratio of the perimeter of the particle $p(S)$ to the perimeter of the equivalent disc. It is related to the excess of interface in respect to the spherical shape. This parameter ranges between 0 and 1 and is equal to 1 for a spherical shape.

$$\varphi = \frac{p(S)}{p(S_c)} \quad (3)$$

2.5 Uniformity η

The Uniformity η measures the difference between the maximum and the minimum distance from the contour of the particle to its gravity centre (respectively r_{max} and r_{min}). This dimensionless parameter is the ratio of the difference explained above to the radius r_0 of the equivalent disc (See Fig.4). The higher is the value of η , the less uniform is the mass distribution around the gravity center. Since a disc is the most uniform particle, η is equal to 0 in this case.

$$\eta = \frac{r_{max} - r_{min}}{r_0} \quad (4)$$

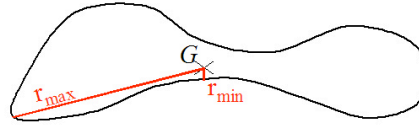


Fig.4. Definition of the Uniformity η

3 Calibration of the shape characterization processing

3.1 The Spherical and Elliptical families

Those four parameters define a shape space and different shape families can be associated to subspaces. The spherical family corresponds to a single point $(\varepsilon, S_p, \varphi, \eta) = (1, 0, 1, 0)$. The elliptical family stands for the droplets having a contour identical to an ellipse. Since the four parameters are related to each other for elliptical drops, this family can be represented by a curve in the 4-D space. Indeed, as an ellipse can be described with only the ε parameter, the three other parameters are related to ε by equations 5 to 7:

$$S_p = \frac{4}{\pi} \left[\arcsin\left(\sqrt{\frac{1}{1+\varepsilon}}\right) - \arcsin\left(\sqrt{\frac{\varepsilon}{1+\varepsilon}}\right) \right] \quad (5)$$

$$\varphi = \left(\frac{3 \cdot (1+\varepsilon)}{4 \cdot \sqrt{\varepsilon}} - \frac{1}{2} \right)^{-1} \quad (6)$$

$$\eta = \frac{1-\varepsilon}{\sqrt{\varepsilon}} \quad (7)$$

Indeed, we can check on Fig.5(a) that a sphere ($\varepsilon = 1$) gives $S_p = 0$ and $\eta = 0$, whereas $\varphi = 1$. For the particular case $\varepsilon = 0$, for which the object is a straight line, $S_p = 2$, η tends toward infinity and φ tends toward 0.

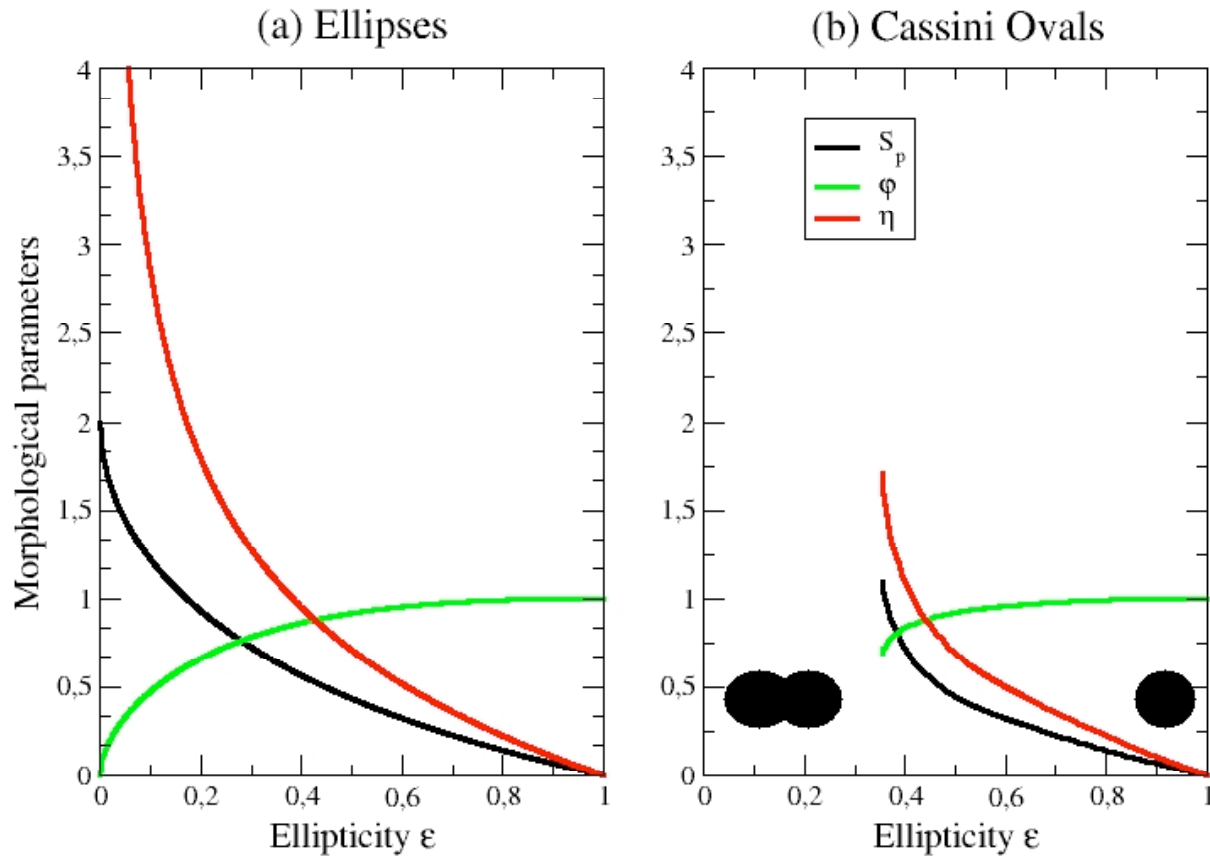


Fig.5. Analytical values of morphological parameters (Sphericity S_p , Irregularity ϕ and Uniformity η) versus Ellipticity ϵ for elliptical family (a) and the Cassini ovals(b).

3.2 The Cassini oval family

3.2.1 Analytical shapes of Cassini ovals

In order to simulate liquid elements submitted to secondary break-up process, we need to define particles of complex shape whose morphological parameters are known. The Cassini ovals are particularly well adapted to simulate drops during fragmentation (secondary break-up). Moreover the shapes described by Cassini ovals cover also droplets whose shape is close to the sphere. As for the elliptical family, the morphological parameters (ϵ , S_p , ϕ , η) of Cassini ovals can be expressed analytically. This feature was used to check the accuracy of our processing programs.

Jean-Dominique Cassini first studied Cassini ovals at the end of the XVII century in order to describe the trajectory of the Earth around the Sun. Nowadays, this curve is used to represent the lines of the magnetic field induced by two parallel wires with same currents passing through them. The lines of the magnetic field are in the orthogonal plane of the two wires, placed in the two focus points of a Cassini oval. This curve can also be seen as the cross section of a tore [4].

This curve gets a symmetry center O and two focus points F and F' equally spaced from the center, as we can see in Fig.7. The characteristic equation of a Cassini oval in cartesian coordinates is given by Equation 8 where $a=OF'=OF$ and $b^2=MF.MF'$ are related to the size of the object:

$$y = \pm \sqrt{\sqrt{4.a^2.x^2 + b^4} - x^2 - a^2} \tag{8}$$

In the following, Cassini oval size and shape are characterized respectively by b and $w=a/b$. Relations between the shape parameters ($\varepsilon, S_p, \varphi, \eta$) of Cassini ovals are given in Fig.5(b). Ellipticity ε for Cassini ovals is limited to 0.35. In fact, for $\varepsilon < 0.35$, the Cassini oval is not anymore a connected surface but is composed of two separated surfaces having the same shape as a pending drop.

As our goal was to describe realistic droplets, w was limited by $0 < w < 1$. $w=1$ corresponds to the Lemniscate of Bernoulli. Examples of Cassini objects of various shapes are shown in Fig.6.

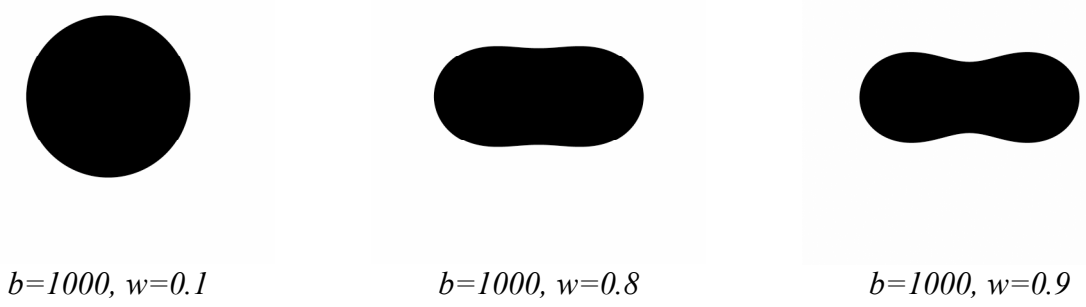


Fig.6. Examples of binary images of various types of Cassini ovals.

In order to check the reliability of our shape characterization processing on real drops, images of Cassini ovals were processed as their shape parameters can be deduced analytically. Cassini ovals images (2048x2048 pixels) were synthesized using Eq. 9. The distance from each pixel (i,j) of the image to the image center was compared to the polar radius $\rho(\theta)$ of Cassini ovals. Pixels inside the perimeter are marked in black and the others are left white.

$$\rho(\theta) = a.\sqrt{\cos(2\theta) \pm \sqrt{w^{-4} - \sin^2(2\theta)}} \quad , \quad 0 < \theta < 2\pi \tag{9}$$

To avoid problems of pixel discretizing for small object compared to the image resolution, a sub-pixel edge detection is used [5]. Indeed, after the simple threshold of a given level, the gray-level gradient around the edge of the object is computed with a Sobel filter. Then, this gradient is used to mark out the sub-pixel contour. Sub-pixel accuracy is useless on binary images like those presented in Fig.6. Indeed, in this case, the grey level gradient is equal to infinity, and thus useless. Even with big object (i.e. with high resolution), the effect of pixel discretizing always occurs, as we can see on the top-left of Fig.7.

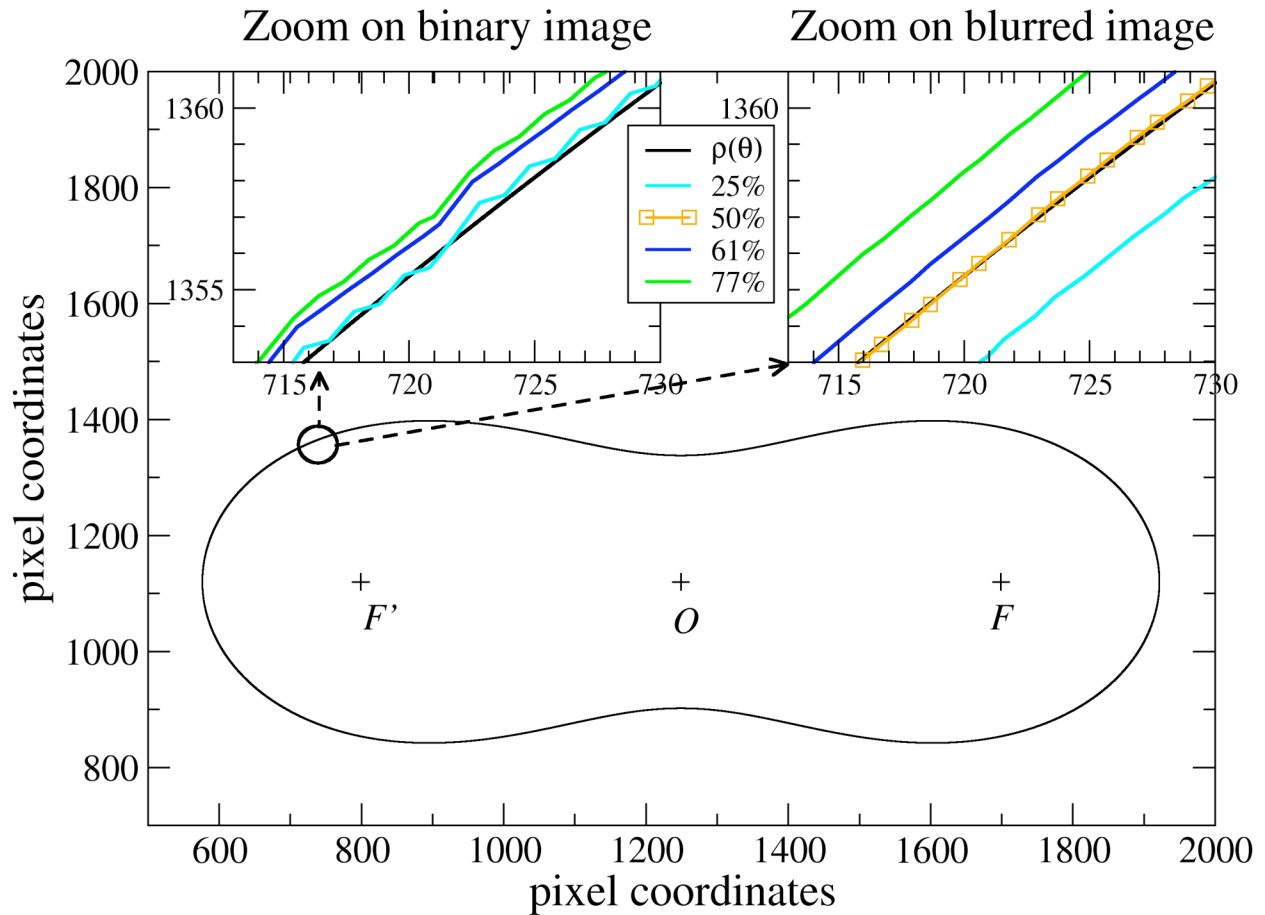


Fig.7. Effect of pixel discretizing on images of Cassini ovals ($b=1000, w=0.9$).

To overcome these limitations, binary images were blurred with a Gaussian kernel of standard deviation equal to 5 pixels. The sub-pixel contour of the Cassini oval is then better described as we can see on the top-right of Fig.7. A threshold level at 50% of the dynamic thus gives the sub-pixel perimeter of the Cassini oval used to compute the morphological parameters.

3.2.2 Comparison between morphological image processing and analytical data

As we can see on Fig.8, the results given by our processing programs on images of Cassini ovals (cross markers) are in a complete agreement with the analytical formulae (black line). The error due to the pixel count is negligible: the error on the Irregularity parameter φ , based on the perimeter, is indeed less than 1%.

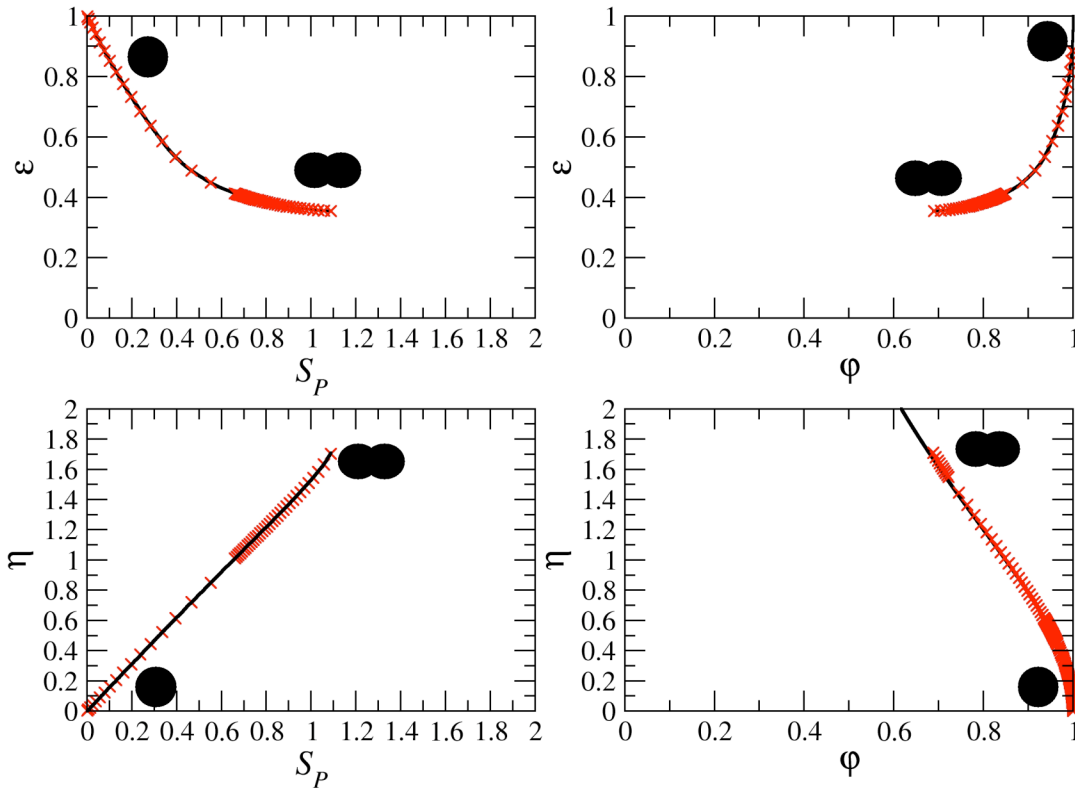


Fig.8. Comparison of image processing (red cross) and analytical computations (black lines) on images of Cassini ovals.

4 Morphological parameters of a fully atomized spray.

The injector used in this study is a commercial 8-holes low-pressure injector used for indirect injection engines. Only the spray produced by 4 of the 8 holes is considered. It is fed with isooctane (2,2,4 trimethylpentane). The injection duration = 5 ms and the injection pressure $p_{inj} = 500$ kPa. Fuel is injected under atmospheric conditions. Measurements are made 60mm from the nozzle, and 7.2 ms after the beginning of the injection, i.e. in a phase of the flow considered to be stationary, in reference to the quasi-constant value of the Sauter Mean Diameter (SMD) for this position ($SMD \approx 250 \mu\text{m}$). Images are made with a shadow-imaging setup compounded of a 10-bit-camera (1200x1600 square pixel of $7.4\mu\text{m}$ side) and a telecentric objective (lateral magnification $\gamma = 1$). The spray is exposed by a short duration flash (12ns).

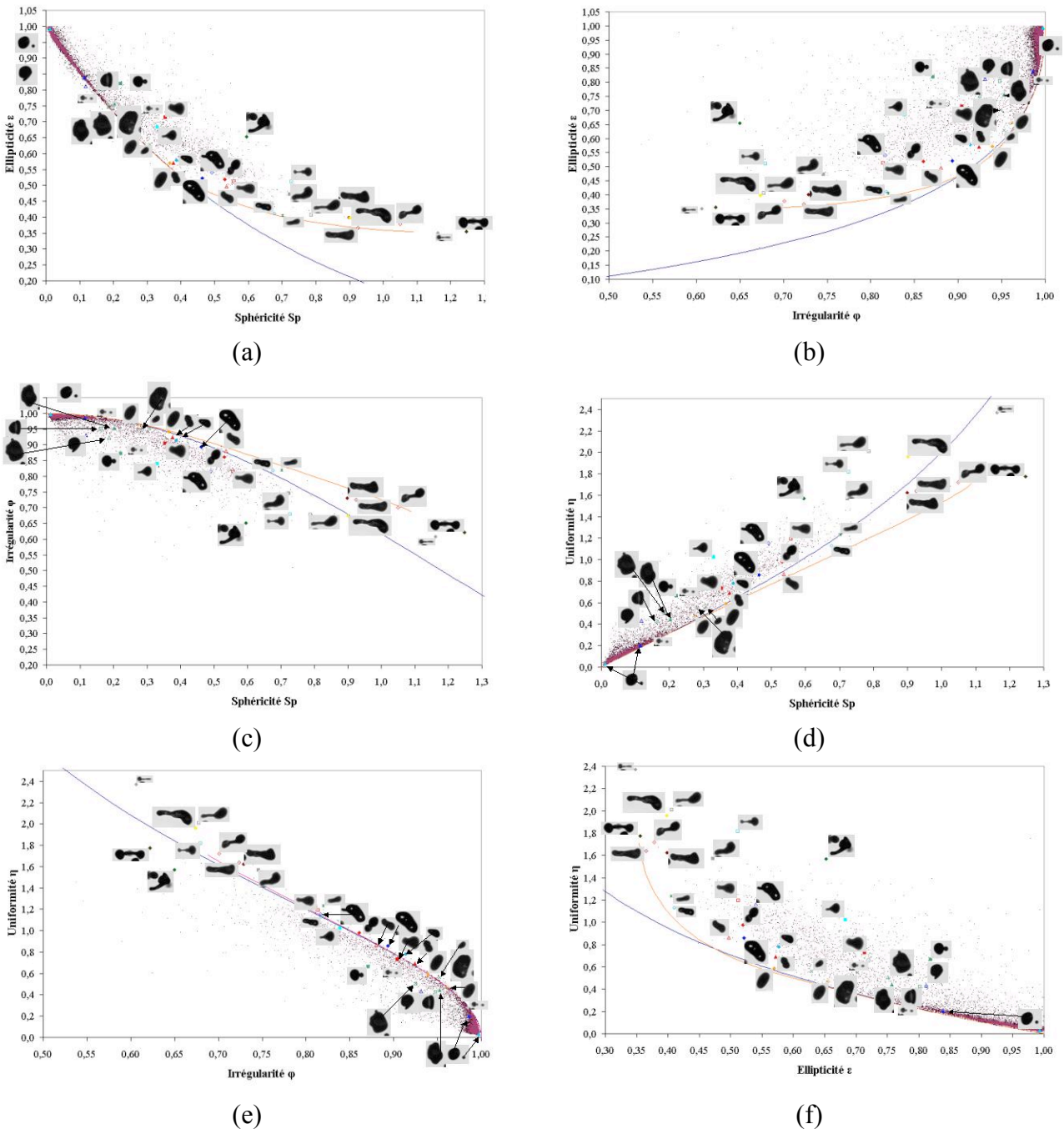


Fig.9. Distribution of the droplets in the shape spaces. The elliptical family is the black line and the Cassini oval family in light orange.

Distributions of the droplets in the morphological spaces are reported in Fig.9. Droplets are mainly located around the elliptical family, particularly for ε close to 1, i.e. for near spherical droplets. The representation in the planes (ε, S_p) , (ε, φ) , (η, ε) , (i.e. Fig.9a, b and f) presents a segmentation of the shapes between ligaments, spherical droplets and other types of droplets like ovoids. When considering droplets of shape far from the sphere, the points in the planes (ε, S_p) , (ε, φ) and (η, ε) move away from the elliptical family, and come closer to the Cassini oval one.

The discrimination between the droplet shapes is not so obvious in the other planes (i.e. (φ, η) , (η, S_p) and (φ, S_p)), as elliptical and Cassini families are close each other. The most complex shapes cannot be associated either to the Cassini or the elliptical family. Cassini and elliptical families are even not separable in the plane (φ, η) , indeed the droplets seem to be aligned along a straight line. These two parameters seem thus to be at least partially redundant. However, the near ligament droplets are located in a sub space of the plane (φ, η) delimited by $(\varphi < 0.8, \eta > 1.2)$.

The investigated spray cannot be considered as fully atomized, as a certain percentage of this droplets are not spherical at all, even if in this region of the spray the mean diameters do not vary significantly. The mean values of the morphological parameters are $(S_p, \varepsilon, \varphi, \eta) = (0.088, 0.9, 0.98, 0.19)$. Those mean values show that most of the droplets are spherical but if we analyze the standard deviation of the morphological parameters $(S_p, \varepsilon, \varphi, \eta) = (0.12, 0.1, 0.05, 0.24)$, we can see that S_p and η vary much more than ε and φ . If we analyze the data given by the couples (ε, S_p) , (ε, φ) , (η, ε) and (φ, η) , most of the droplets are found to be close to the elliptical family, particularly for the near-spherical droplets. Droplets whose shape is more complex ($\varepsilon < 0.5$, $S_p > 0.5$, $\varphi > 0.9$, $\eta > 0.5$) have their shape parameters moving away from the elliptical family and moving closer to the Cassini oval family.

Conclusion & future works

Droplet shapes are not confined to the only spherical element, especially prior to the complete atomization of the spray. In such cases, mean diameters like SMD are not enough to properly quantify the state of the spray. An Imaging technique is used in this context to analyze the drop shapes. New analysing tools for the characterization of the liquid elements during atomization has been described in this paper.

4 morphological parameters $(S_p, \varepsilon, \varphi, \eta)$ describe the droplet shapes. Analytical values of those parameters have been formulated for Elliptical and Cassini oval families because their shapes well simulate the droplets during the secondary break-up process.

The morphological analysing tool have been tested on synthesized images of Elliptical objects and Cassini ovals. The comparison between analytical data and image processing confirmed the reliability of the technique.

The morphological analysis have been performed on a spray produced by a commercial low pressure gasoline injector. The distributions of the droplets in the different shape spaces defined by the planes (ε, S_p) , (ε, φ) , (η, ε) , and (φ, η) show that most of the drops are located around the Elliptical family. Droplets of more complex shape move away from the elliptical family and come closer to the Cassini oval one, particularly for the representation in the planes (ε, S_p) , (ε, φ) , and (η, ε) . There is thus a segmentation of the shapes between ligaments, spherical droplets and other types of droplets like ovoids. It is also noticed that droplets seem to be aligned along a straight line in the plane (φ, η) , indicating that these two parameters seem to be partially redundant.

Future works are scheduled to quantify the displacements of droplets not fully atomized in the shape spaces and to analyze the variation of the mean morphological parameters during the atomization process. Moreover, it will be checked if this method could help to clearly identify complex liquid elements such as ligaments in the very beginning of the secondary break-up.

References

1. Chigier N. Optical Imaging of Sprays. *Prog. Energy Combust. Sci.*, Vol. 17, pp 211-262, 1991.
2. Malot H and Blaisot J.B. Droplet Size distribution and Sphericity Measurements of Low-Density Sprays through Image Analysis, *Part. Part. Syst. Charact.* No. 17, pp 146-158, 2000.
3. Malot H and Dumouchel C. Experimental investigation of drop-size distribution of sprays produced by a low-velocity Newtonian cylindrical liquid jet, *Atomization and Sprays*, Vol. 11, pp 227-254, 2001.
4. <http://www.mathcurve.com/courbes2d/cassini/cassini.shtml>
5. Yon J. "Jet Diesel haute pression en champ proche : étude par imagerie", *thesis*, Rouen, 2004.

Copyright Statement

The authors confirm that they, and/or their company or institution, hold copyright on all of the original material included in their paper. They also confirm they have obtained permission, from the copyright holder of any third party material included in their paper, to publish it as part of their paper. The authors grant full permission for the publication and distribution of their paper as part of the ISFV13/FLUVISU12 proceedings or as individual off-prints from the proceedings.